THE JOURNAL OF BIOLOGICAL CHEMISTRY VOL. 289, NO. 12, pp. 8312–8325, March 21, 2014

The 2-Oxoacid Dehydrogenase Complexes in Mitochondria Can Produce Superoxide/Hydrogen Peroxide at Much Higher Rates Than Complex I*

Received for publication, December 23, 2013, and in revised form, January 16, 2014 Published, JBC Papers in Press, February 10, 2014, DOI 10.1074/jbc.M113.545301

Casey L. Quinlan[‡1], Renata L. S. Goncalves[‡], Martin Hey-Mogensen[‡§2], Nagendra Yadava[¶], Victoria I. Bunik[‖], and Martin D. Brand[‡3]

From [‡]The Buck Institute for Research on Aging, Novato, California 94945, [§]Department of Biomedical Sciences, Center for Healthy Aging, Copenhagen University, Copenhagen DK-2200, Denmark, [¶]Pioneer Valley Life Sciences Institute, Springfield, Massachusetts 01107, and [‖]A. N. Belozersky Institute of Physico-Chemical Biology and Faculty of Bioengineering and Bioinformatics, Lomonosov Moscow State University, Moscow 119991, Russia

Background: At the redox potential of NADH/NAD^+, at least four mitochondrial sites produce superoxide/H_2O_2.
Results: We compare their capacities *in situ* in isolated mitochondria.
Conclusion: Maximum capacities of complexes were 2-oxoglutarate dehydrogenase > pyruvate dehydrogenase > branched-chain 2-oxoacid dehydrogenase > complex I.
Significance: H_2O_2 production from 2-oxoacid dehydrogenases can be considerable but may previously have been misattributed to complex I.

Several flavin-dependent enzymes of the mitochondrial matrix utilize NAD^+ or NADH at about the same operating redox potential as the NADH/NAD^+ pool and comprise the NADH/NAD^+ isopotential enzyme group. Complex I (specifically the flavin, site I_F) is often regarded as the major source of matrix superoxide/H_2O_2 production at this redox potential. However, the 2-oxoglutarate dehydrogenase (OGDH), branched-chain 2-oxoacid dehydrogenase (BCKDH), and pyruvate dehydrogenase (PDH) complexes are also capable of considerable superoxide/H_2O_2 production. To differentiate the superoxide/H_2O_2-producing capacities of these different mitochondrial sites *in situ*, we compared the observed rates of H_2O_2 production over a range of different NAD(P)H reduction levels in isolated skeletal muscle mitochondria under conditions that favored superoxide/H_2O_2 production from complex I, the OGDH complex, the BCKDH complex, or the PDH complex. The rates from all four complexes increased at higher NAD(P)H/$NAD(P)^+$ ratios, although the 2-oxoacid dehydrogenase complexes produced superoxide/H_2O_2 at high rates only when oxidizing their specific 2-oxoacid substrates and not in the reverse reaction from NADH. At optimal conditions for each system, superoxide/H_2O_2 was produced by the OGDH complex at about twice the rate from the PDH complex, four times the rate from the BCKDH complex, and eight times the rate from site I_F of complex I. Depending on the substrates present, the dominant sites of superoxide/H_2O_2 production at the level of NADH may be the OGDH and PDH complexes, but these activities may often be misattributed to complex I.

Mitochondria may generate superoxide anion radical ("superoxide") or H_2O_2 from at least 10 distinct sites in the electron transport chain and associated pathways (such as the Krebs cycle and β-oxidation). Respiratory complexes I and III are usually described as the principal producers (1–9), but many other mitochondrial enzymes can also reduce oxygen prematurely, most notably complex II (10).

In complex I there are two sites of superoxide production: the flavin in the NADH-oxidizing site (site I_F)[4] and the ubiquinone-reducing site (site I_Q) (11). In complex III, superoxide arises from the quinol-oxidizing site (site III_{Qo}) (12–14). In complex II, the flavin site of complex II (site II_F) generates superoxide and/or H_2O_2 (10). Other sites include mitochondrial glycerol-3-phosphate dehydrogenase (15), the electron transferring flavoprotein/ETF:ubiquinone oxidoreductase system of fatty acid β-oxidation (16), dihydroorotate dehydrogenase (15, 17), and the dihydrolipoamide dehydrogenase of 2-oxoacid dehydrogenase complexes (18): 2-oxoglutarate dehydrogenase (OGDH) complex

* This work was supported, in whole or in part, by National Institutes of Health Grant TL1 AG032116 (to C. L. Q.). This work was also supported by The Ellison Medical Foundation Grant AG-SS-2288-09 (to M. D. B.), the Brazilian Government through the Coordenação de Aperfeiçoamento de Pessoal de Nível Superior (CAPES) e ao Conselho de Nacional de Desenvolvimento Científico e Tecnológico programa Ciências Sem Fronteiras (CNPq-CSF) (to R. L. S. G.), the Carlsberg Foundation (to M. H.-M.), the Center for Excellence in Apoptosis Research funds from Massachusetts Technology Collaborative Grant A00000000004448 (to N. Y.), and Russian Foundation of Basic Research (RFBR) Grant 12-04-01541 (to V. I. B.).
[1] Present address: Oncology Research Unit, Pfizer Inc., La Jolla, CA 92121.
[2] Present address: Dept. of Diabetes NBEs and Obesity Biology, Novo Nordisk A/S, DK-2760 Måløv, Denmark.
[3] To whom correspondence should be addressed: Buck Institute for Research on Aging, 8001 Redwood Blvd., Novato, CA 94945. Tel.: 415-493-3676; Fax: 415-209-2235; E-mail: mbrand@buckinstitute.org.

[4] The abbreviations used are: site I_F, flavin in the NADH-oxidizing site of complex I; site I_Q, ubiquinone-reducing site of complex I; site II_F, flavin site of complex II; site III_{Qo}, quinol-oxidizing site of complex III; OGDH, 2-oxoglutarate dehydrogenase; PDH, pyruvate dehydrogenase; BCKDH, branched-chain 2-oxoacid (or α-ketoacid) dehydrogenase; KMV, 3-methyl-2-oxopentanoate (α-keto-methylvalerate); KIV, 3-methyl-2-oxobutanoate (α-keto-isovalerate); KIC, 4-methyl-2-oxopentanoate (α-ketoisocaproate); E_h, operating redox potential; Q, ubiquinone; QH_2, ubiquinol; E1, 2-oxoacid dehydrogenase; E2, dihydrolipoamide acyltransferase; E3, dihydrolipoamide dehydrogenase; PDP, pyruvate dehydrogenase phosphatase; ETF, electron transferring flavoprotein.

(19–21), branched-chain 2-oxoacid dehydrogenase (BCKDH) complex (22), and pyruvate dehydrogenase (PDH) complex (20, 23). Proline dehydrogenase has also been implicated (24). Most studies on mitochondrial production of superoxide and H_2O_2 have concentrated on the maximum capacities of one or other of these sites when electron flow is blocked by electron transport chain inhibitors, but techniques to assay the rates from several different sites during normal electron flow are now becoming available (15, 16, 25–27).

Complex I is often credited as the primary site of matrix superoxide production when electron flow from Krebs cycle intermediates into the rest of the respiratory chain is inhibited by the addition of rotenone to block site I_Q (1–9). However, other sites within the matrix can also be important producers of superoxide/H_2O_2 under these conditions (19, 20, 23). Together with site I_F, these matrix sites (including the OGDH, BCKDH, and PDH complexes) comprise the NADH/NAD^+ isopotential group, *i.e.* they operate at the relatively low redox potential of the NADH/NAD^+ pool. The matrix sites are flavoenzymes. Reduced flavins are good electron donors to oxygen (28), as shown for several isolated flavoenzymes (19, 20, 29, 30). The relative contribution of each site in the NADH/NAD^+ isopotential group to superoxide/H_2O_2 production by isolated mitochondria has not been measured. This may be because they probably all respond to the reduction state of the NADH pool, making it hard to assign individual activities.

The objective of the present study was to measure the relative maximum capacities for superoxide/H_2O_2 production of the matrix NADH/NAD^+-linked enzyme complexes OGDH, BCKDH, PDH, and complex I under optimal conditions *in situ* in isolated muscle mitochondria. We show that complex I is not the highest capacity matrix superoxide/H_2O_2-producing enzyme in the presence of rotenone. Instead, the OGDH complex has the greatest capacity followed by the PDH complex and the BCKDH complex. Site I_F of complex I has the lowest capacity in this isopotential group.

EXPERIMENTAL PROCEDURES

Animals, Mitochondria, and Reagents—Female Wistar rats (Harlan Laboratories), age 5–8 weeks, were fed chow *ad libitum* and given free access to water. Mitochondria were isolated from hind limb skeletal muscle at 4 °C in Chappell-Perry buffer (CP1; 100 mM KCl, 50 mM Tris, 2 mM EGTA (pH 7.4 at 4 °C) by standard procedures (31). The animal protocol was approved by the Buck Institute Animal Care and Use Committee (IACUC) in accordance with IACUC standards. All reagents were from Sigma except Amplex UltraRed (Invitrogen) and atpenin A5 (Santa Cruz).

Complex I-deficient mutant (*Ndufa1*$^{S55A/Y}$) and wild-type control (*Ndufa1*$^{+/Y}$) male mice were used at 24 weeks of age. Mutant mice were developed by *Ndufa1*^{S55A} allele knock-in at the native locus by homologous recombination on the X chromosome on the 129/Sv genetic background.[5] Animals were fed *ad libitum* and given free access to water. Mitochondria were isolated from hind limb skeletal muscle as above (31), except tissue was disrupted with no more than five strokes in a glass-Teflon homogenizer. Mitochondria were resuspended in CP1, and protein was measured by the biuret method.

Superoxide/H_2O_2 Production—Rates of superoxide/H_2O_2 production were measured collectively as rates of H_2O_2 production, as two superoxide molecules are dismutated by endogenous or exogenous superoxide dismutase to yield one H_2O_2. H_2O_2 was detected using horseradish peroxidase and Amplex UltraRed (9). Mitochondria (0.3 mg of protein·ml^{-1}) were suspended at 37 °C in non-phosphorylating medium containing 120 mM KCl, 5 mM Hepes, 5 mM KH_2PO_4, 2.5 mM $MgCl_2$, 1 mM EGTA, 0.3% (w/v) bovine serum albumin (pH 7.0 at 37 °C), 5 units·ml^{-1} horseradish peroxidase, 25 units·ml^{-1} superoxide dismutase, 50 μM Amplex UltraRed, and 1 μg·ml^{-1} oligomycin. For measurement of H_2O_2 production from the PDH complex, the medium also contained 1 mM dichloroacetic acid and 450 nM free Ca^{2+} (achieved by addition of 575 μM total Ca^{2+}, calculated using the program MaxChelator). Reactions were monitored fluorometrically in a Varian Cary Eclipse spectrofluorometer ($\lambda_{excitation}$ = 560 nm, $\lambda_{emission}$ = 590 nm) with constant stirring and calibrated with known amounts of H_2O_2 in the presence of all relevant substrates, as some substrates quenched the fluorescence (9).

H_2O_2 production rates in Fig. 11 were corrected for losses of H_2O_2 caused by peroxidase activity in the matrix to give a better estimate of actual superoxide/H_2O_2 production rates. Rates were mathematically corrected to those that would have been observed in these mitochondria after pretreatment with 1-chloro-2,4-dinitrobenzene to deplete glutathione and decrease glutathione peroxidase and peroxiredoxin activity as described (27, 32) using an empirical equation,

$$\nu_{CDNB} = \nu_{control} + (1.43\nu_{control}/(0.55 + \nu_{control})) \quad \text{(Eq. 1)}$$

where rates are in nmol H_2O_2·min^{-1}·mg of $protein^{-1}$.

NAD(P)H Redox State—Experiments used 0.3 mg of mitochondrial protein·ml^{-1} at 37 °C in parallel with measurements of H_2O_2 production in the same non-phosphorylating medium with the same additions. The reduction state of endogenous NAD(P)H was determined by autofluorescence (most of the signal is from NADH bound in the matrix, and NADPH hardly changes in the present experiments, but for full disclosure we call it "NAD(P)H") using a Shimadzu RF5301-PC at $\lambda_{excitation}$ = 365 nm, $\lambda_{emission}$ = 450 nm (11, 27). NAD(P)H was assumed to be 0% reduced after 5 min without added substrate and 100% reduced with saturating substrate (*e.g.* 5 mM malate plus 5 mM glutamate) and 4 μM rotenone. Intermediate values were determined as % reduced NAD(P)H relative to the 0 and 100% values. 3-Methyl-2-oxopentanoate (α-keto-methylvalerate (KMV)) decreased the NAD(P)H signal. To correct for this, 3-methyl-2-oxopentanoate was titrated from 0–20 mM, and the dependence of fluorescence on 3-methyl-2-oxopentanoate concentration was determined. The corrected fluorescence l_o was calculated as $l_o = 10^{(C\times slope)}\times l$, where l = observed fluorescence, and C = 3-methyl-2-oxopentanoate concentration.

Permeabilized Mitochondria—Mitochondria were permeabilized with alamethicin according to Grivennikova *et al.* (33). Intact mitochondria (25–35 mg of protein·ml^{-1}) were diluted 20-fold with medium at 25 °C comprising 0.25 M sucrose, 10

[5] C. Kim and N. Yadava, unpublished data.

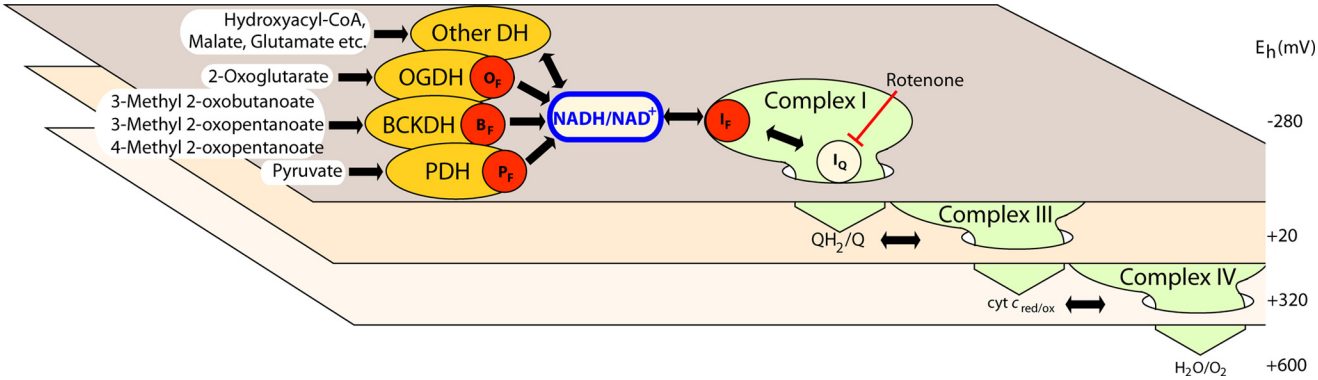

FIGURE 1. **The NADH/NAD$^+$ isopotential group and its component superoxide/H_2O_2-producing enzymes.** The three planes represent different isopotential groups of redox centers in mitochondria. Each group contains multiple redox centers operating at about the same redox potential (E_h): centers around NADH/NAD$^+$ at $E_h \sim -280$ mV, around QH_2/Q at $E_h \sim +20$ mV, and around cytochrome *c* at $E_h \sim +320$ mV (34). The normal flow of electrons from substrate dehydrogenases through NADH and the respiratory complexes of the electron transport chain to oxygen are indicated by the large *green arrows* dropping down through the isopotential planes. Electrons from NAD-linked substrates enter the NADH/NAD$^+$ pool at $E_h \sim -280$ mV through NAD-linked dehydrogenases (*DH*) including the OGDH, BCKDH, and PDH complexes and flow into complex I (site I_F). In the absence of rotenone they then drop down via site I_Q to QH_2/Q in the next isopotential pool through complex III to cytochrome *c* and ultimately to their final acceptor, oxygen. In the presence of rotenone (*red blunted arrow*) other sites of superoxide and H_2O_2 production are fully oxidized and, therefore, do not leak electrons to O_2, and only the sites in the NADH/NAD$^+$ isopotential pool are active. These sites (*red dots*) are site I_F, the flavin of the OGDH complex (O_F), the flavin of the BCKDH complex (B_F), and the flavin of the PDH complex (P_F) (see Ref. 26).

mM Hepes/KOH (pH 7.4), 0.2 mM EDTA, bovine serum albumin (1 mg·ml^{-1}), 2.5 mM $MgCl_2$, and alamethicin (40 μg·ml^{-1}). The suspension was incubated for 5 min, diluted 2.5-fold with the same buffer but ice-cold and lacking $MgCl_2$ and alamethicin, then centrifuged at 30,000 × *g* for 15 min. The permeabilized mitochondria were suspended in 0.25 M sucrose, 10 mM HEPES (pH 7.4), 0.2 mM EDTA, and 10 mg · ml^{-1} bovine serum albumin and stored on ice.

Complex I Activity—NADH:quinone oxidoreductase activity was assayed at 30 °C as a decrease of A_{340} with 100 μM NADH as substrate and 100 μM ubiquinone-1 (Q_1) as acceptor in the presence of 1 mM KCN (33) in medium comprising 0.25 M sucrose, 10 mM HEPES (pH 7.4), 0.2 mM potassium EDTA, and permeabilized mitochondria (0.125 mg of protein·ml^{-1}). A_{340} was measured in an Olis DW2 dual-beam spectrophotometer in split beam mode. The rotenone-sensitive linear rates of NADH oxidation over 60 s were converted to molar units with $\epsilon = 6.22$ mM·cm^{-1}.

Western Blot—To determine the amount of complex I, 0.4 μg of mitochondrial protein was boiled in NU-PAGE loading buffer. Proteins were separated by 4–12% NU-PAGE gradient gel using 1× MES buffer (Invitrogen) and transferred to a nitrocellulose membrane. Anti-complex I 75-kDa subunit (NDUFS1) (Santa Cruz: sc-271510) was used at a 1:1000 dilution. Secondary antibody was horseradish peroxidase-conjugated goat anti-mouse (Bio-Rad) at 1:50,000 dilution. Chemiluminescence was generated with SuperSignal West Pico (Thermo Scientific) and quantified with Image J software (National Institutes of Health).

RESULTS AND DISCUSSION

The aim of this study was to determine the relative maximum capacities of different matrix sites of superoxide/H_2O_2 production in the NADH/NAD$^+$ isopotential group in intact skeletal muscle mitochondria. Electrons leak from the respiratory chain to generate superoxide or H_2O_2 at two different redox potentials (E_h): at the isopotential group of redox carriers around the NADH/NAD$^+$ pool at $E_h \sim -280$ mV and at the isopotential group of redox carriers around the QH_2/Q pool at $E_h \sim +20$ mV (26, 27, 34) (Fig. 1). At each isopotential group, an important determinant of the rate of superoxide or H_2O_2 production is the redox state; the more reduced species will generally leak electrons to oxygen at a faster rate.

The NADH/NAD$^+$ isopotential group contains several enzymes, but of interest here are the superoxide/H_2O_2 producing enzymes, which are typically flavoenzymes. Reduced flavins and flavoproteins generate radicals (19, 20, 28). In particular, the flavin sites of complex I (site I_F) and the OGDH complex may be important sources of matrix superoxide/H_2O_2 (19, 20, 30). There is no evidence that the BCKDH complex produces superoxide or H_2O_2, but it shares with the other 2-oxoacid dehydrogenase complexes a dihydrolipoamide dehydrogenase subunit that is likely a source of superoxide/H_2O_2 production. Isolated PDH complex generates superoxide/H_2O_2 (20, 23), but the physiological relevance is uncertain. Other members of the NADH/NAD$^+$ isopotential group, such as malate dehydrogenase and isocitrate dehydrogenase, have not been shown to produce superoxide or H_2O_2 (35). Here we describe conditions under which complex I and the OGDH, BCKDH, and PDH complexes are largely distinct from each other, analyze the conditions required for maximum rates in skeletal muscle mitochondria, and compare the maximum rates of superoxide/H_2O_2 production by each complex.

Complex I Flavin (Site I_F)—Complex I (NADH-ubiquinone oxidoreductase) oxidizes NADH to NAD$^+$ and reduces ubiquinone (Q) to ubiquinol (QH_2). During this process two electrons are transferred through multiple redox centers, and four protons are pumped from the matrix to the intermembrane space. The enzyme is fully reversible, either oxidizing NADH and reducing Q (and pumping protons) in the forward reaction or oxidizing QH_2 and reducing NAD$^+$ in the reverse reaction driven by protonmotive force (34).

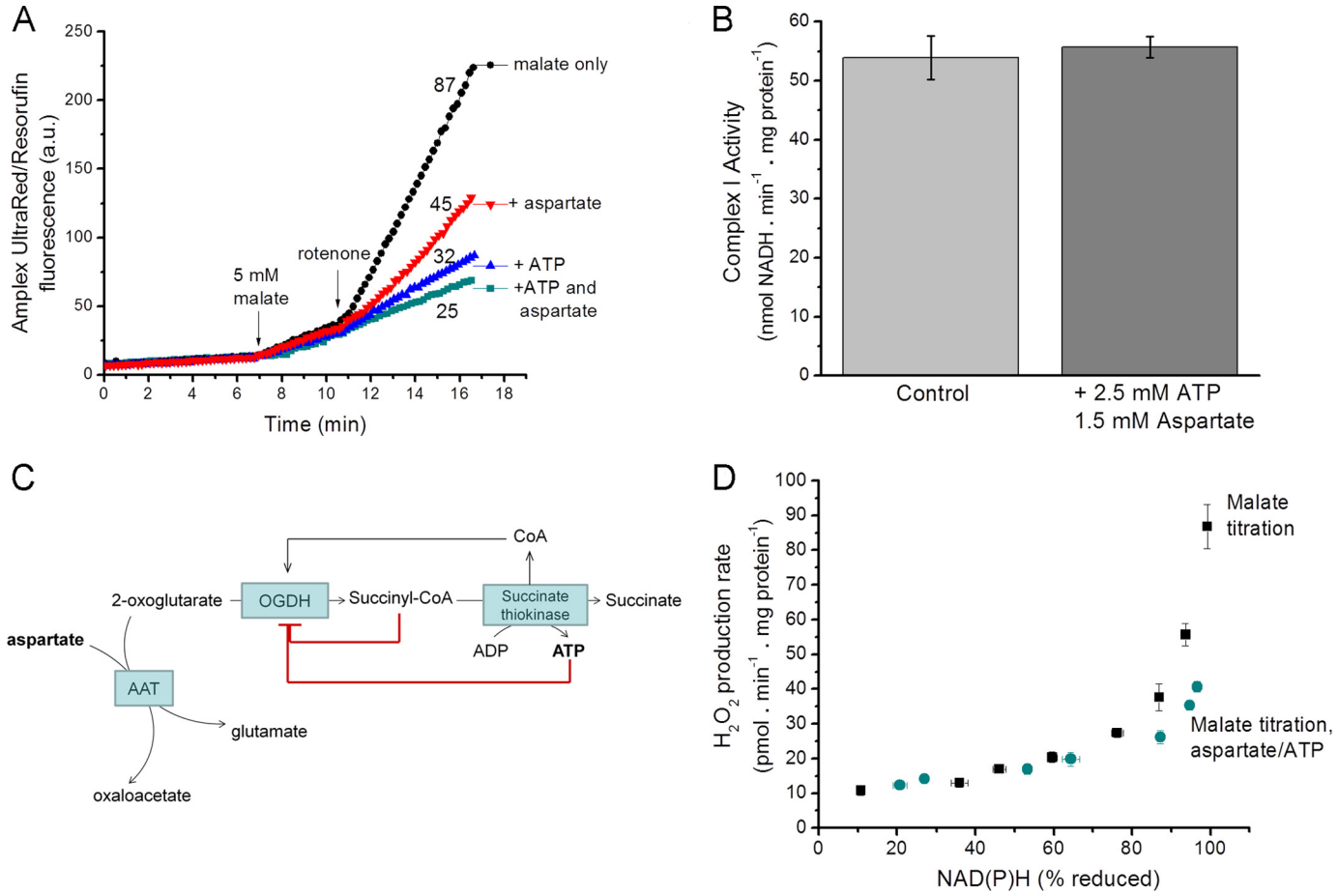

FIGURE 2. **Superoxide/H_2O_2 production with malate as substrate; complex I and the OGDH complex.** *A*, Amplex UltraRed traces illustrate that H_2O_2 production rates with 5 mM malate as substrate were decreased by the addition of 2.5 mM ATP and 1.5 mM aspartate. Mitochondria were suspended in non-phosphorylating medium, and 4 μM rotenone was added where indicated. A representative trace is shown; *numbers* indicate mean rates in pmol of H_2O_2·min^{-1}·mg of protein^{-1} from four replicates. *a.u.*, arbitrary units. *B*, complex I activity measured in alamethicin-permeabilized mitochondria as the rotenone-sensitive NADH:Q-oxidoreductase activity at 30 °C was unaffected by addition of ATP plus aspartate. *C*, schematic to illustrate that in isolated mitochondria ATP and aspartate may indirectly inhibit the OGDH complex by decreasing its substrates 2-oxoglutarate (through aspartate aminotransferase (*AAT*)) and CoA (through inhibition of succinate thiokinase), increasing its inhibitory product succinyl CoA (through inhibition of succinate thiokinase) and through direct inhibitory effects of ATP on the enzyme. *D*, dependence of superoxide/H_2O_2 production on the redox state of NAD(P)H (measured by autofluorescence). Malate was titrated from 20 μM–5 mM in the presence of 4 μM rotenone either in the presence or absence of 1.5 mM aspartate and 2.5 mM ATP. Data in *A* are representative traces. Data in *B* and *D* are the means ± S.E. ($n = 3$).

Complex I produces superoxide at two different internal sites: the NADH-oxidizing flavin site, I_F, and the ubiquinone-reducing site, I_Q (11, 36–40), although site I_Q activity has yet to be measured in the reconstituted complex (41). The production of superoxide from site I_F occurs when electrons leak to O_2 from the fully reduced flavin, $FMNH_2$ (30). As electrons can only be transferred to oxygen when the flavin is reduced, it is likely that the steady-state concentration of reduced $FMNH_2$ is an important determinant of the rate of superoxide production from this site. Similarly, the steady-state reduction level of FMN depends on the steady-state redox state of its reductant, NADH (*i.e.* the NADH/NAD^+ ratio). Therefore, the steady-state reduction level of NADH/NAD^+ *in situ* predicts the rate of superoxide production from site I_F (27). Indeed, as the NAD(P)H/$NAD(P)^+$ ratio increases, the rate of superoxide production attributed to site I_F in complex I increases steeply (26, 27, 32).

The relationship between superoxide/H_2O_2 production from site I_F and the reduction state of NAD(P)H can be revealed by titrating mitochondria with a substrate that reduces NAD^+ in the presence of rotenone to prevent its rapid reoxidation (*squares*, Fig. 2*D*). Malate was chosen here because malate dehydrogenase is thought to reduce NAD^+ directly without generating superoxide or H_2O_2 (35) or providing sufficient Krebs cycle intermediates to support superoxide/H_2O_2 production from other sites. To test the robustness of the relationship between superoxide produced from site I_F and NAD(P)H reduction state, we added physiologically relevant components such as amino acids and nucleotides to the medium. In general, this did not change the established relationship between the observed rate of H_2O_2 production and the NAD(P)H reduction level (*squares*, Fig. 2*D*). However, the addition of two biologically relevant compounds, ATP and aspartate, decreased the observed rate of mitochondrial H_2O_2 production (Fig. 2*A*) without changing the reduction state of NAD(P)H (Fig. 2*D*) or the NADH:Q oxidoreductase activity of complex I (Fig. 2*B*).

ATP and aspartate may affect other matrix enzymes, for example the OGDH complex (Fig. 2*C*). ATP is a negative regulator of many Krebs cycle enzymes, including OGDH (42, 43). It may also product-inhibit succinate thiokinase, which generates

succinate and ATP from succinyl-CoA (44); thus, ATP will lower free CoA, a substrate for the OGDH complex, and raise succinyl-CoA, a potent product inhibitor of the complex (45). Aspartate will drive the aspartate aminotransferase reaction, aspartate + 2-oxoglutarate ↔ oxaloacetate + glutamate, to remove 2-oxoglutarate. To check this, we inhibited aminotransferases using aminooxyacetate, which eliminated the effect of aspartate addition (not shown). Thus, the effects of aspartate and ATP on mitochondrial H_2O_2 production point to 2-oxoglutarate and CoA-dependent production of superoxide by the OGDH complex in the physiological (forward) reaction (19). The non-additivity of the effects of aspartate and ATP (Fig. 2*A*) supports this conclusion, as they each affect the same process (Fig. 2*C*).

We found no other agents that further decreased the rate of H_2O_2 production driven by oxidation of malate in the presence of rotenone, so we assume that the residual rate in the presence of ATP and aspartate (Fig. 2*D*) was solely attributable to site I_F (any NADH-dependent contribution from dihydrolipoamide dehydrogenase (18) under these conditions would also be included in our measurements of H_2O_2 production by site I_F). Therefore, the lower set of points in Fig. 2*D* can be used to predict the rate from site I_F at any measured reduction state of NAD(P)H *in situ*.

The maximum observed rates of H_2O_2 production from site I_F in muscle mitochondria when NAD^+ is highly reduced occur when the size of the NADH+NAD^+ pool and the concentrations of other effectors are set by the system. These rates may be very different from the maximum rates achievable with the isolated enzyme (30) or in submitochondrial particles (46, 47), where the concentrations of effectors can be independently optimized. The same argument applies to the other sites analyzed below. When comparing the capacities of different sites *in situ*, the maximum rates in intact mitochondria are more relevant.

Based on the logic outlined above, we propose that the effects of ATP and aspartate on the rate of H_2O_2 production with malate as substrate were mediated by effects on the OGDH complex, not direct effects on complex I. Furthermore, the OGDH complex may often be the predominant source of superoxide/H_2O_2 when classical complex I substrate mixes are used.

2-Oxoacid Dehydrogenase Complexes—The 2-oxoacid dehydrogenase complexes catalyze the oxidation of 2-oxoacids (2-oxoglutarate, branched-chain 2-oxoacids, or pyruvate) to yield the corresponding acyl-CoAs and NADH. Multiple copies of three enzymatic components are organized into complexes (48). The first reaction is the irreversible decarboxylation of the 2-oxoacid, catalyzed by a specific 2-oxoacid dehydrogenase (E1) that requires the cofactor thiamine pyrophosphate. The second reaction is catalyzed by dihydrolipoamide acyltransferase (E2) and requires CoA to generate an acyl-CoA. The third reaction is catalyzed by dihydrolipoamide dehydrogenase (E3) and requires FAD^+ and NAD^+ to reoxidize the dihydrolipoamide. E1 and E2 are unique to the individual complexes, but E3 is the same gene product in each complex and catalyzes an identical reaction (49); it is also present in the glycine cleavage system. The covalently attached lipoate group in E2 connects

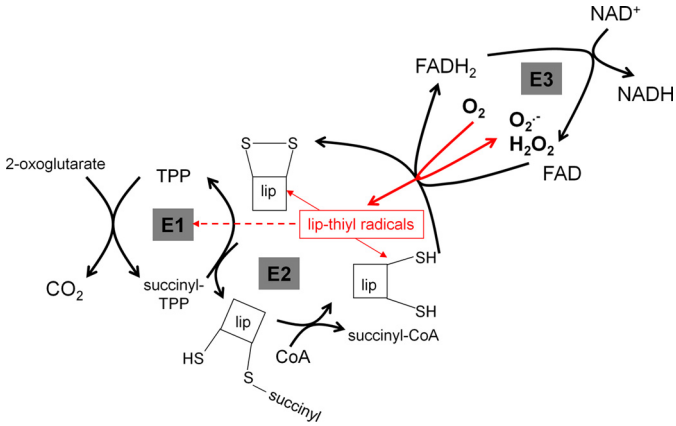

FIGURE 3. **Generation of superoxide and H_2O_2 by the 2-oxoglutarate dehydrogenase complex.** The complex contains multiple copies of the three major components: thiamin pyrophosphate (*TPP*)-dependent E1, E2, which contains the lipoyl group (*lip*), and E3, which contains FAD. Side reactions involving the E3-bound FAD and the E2-bound lipoyl residues when NAD is limiting are shown in *red*. Oxidation of $FADH_2$ by O_2 can generate superoxide or H_2O_2 (19–21). When it generates superoxide, the resulting FADH* can reduce lipoyl residues to thiyl radicals (19, 50), which may inactivate E1 (*dashed line*) or dismutate (*arrows to the reduced and oxidized lipoyl species*).

the three active sites of E1, E2, and E3 and channels substrates through the complexes. E2 forms the catalytic core and establishes the structural foundation for the complex, as both E1 and E3 bind to it.

2-Oxoglutarate Dehydrogenase Complex—The OGDH complex catalyzes the conversion of 2-oxoglutarate to succinyl-CoA in the Krebs cycle. The mammalian enzyme is regulated by ATP, ADP, calcium, and substrate availability. It is inhibited by its products, succinyl-CoA and NADH (42, 43).

The OGDH complex is an important source of reactive oxygen species in the matrix (19–21, 50, 51). It is a major source of H_2O_2 in isolated brain mitochondria at high NADH/NAD^+ (20, 21, 52) and of superoxide in neurons during glutamate excitotoxicity (51). The E3 component of the purified enzyme contains the redox-active flavin that reduces oxygen (53, 54) and generates substantial superoxide/H_2O_2 when NAD^+ is limiting (19–21). E3 is abundant in skeletal muscle mitochondria (55), and the midpoint potential of the flavin is sufficiently negative (~−280 mV) to make it a good electron donor to oxygen (56).

When E3 functions within the OGDH or PDH complexes, the reduced lipoyl residue may equilibrate with the FADH* semiquinone formed by $1e^-$ oxidation of $FADH_2$ by O_2. Because of this, formation of superoxide by E3 is associated with generation of lipoate thiyl radicals (19, 50) (Fig. 3). This side reaction may occur when FAD is reduced in either the forward reaction (from 2-oxoglutarate oxidation in the presence of CoA leading to reduction of the dihydrolipoyl residue) or the reverse reaction (from NADH oxidation). Efficient addition of O_2 to thiyl radicals has not been observed (57), but thiyl radicals are very reactive species, which in the case of the OGDH and PDH complexes, are more damaging than superoxide/H_2O_2 (19). Intrinsic thiyl radical formation underlies an important regulatory mechanism in the OGDH and PDH complexes, irreversibly inactivating the corresponding E1s when NAD^+ is lacking (19, 50). Inactivation is favored by particular matrix environments, *e.g.* the reduced state of NADH, and

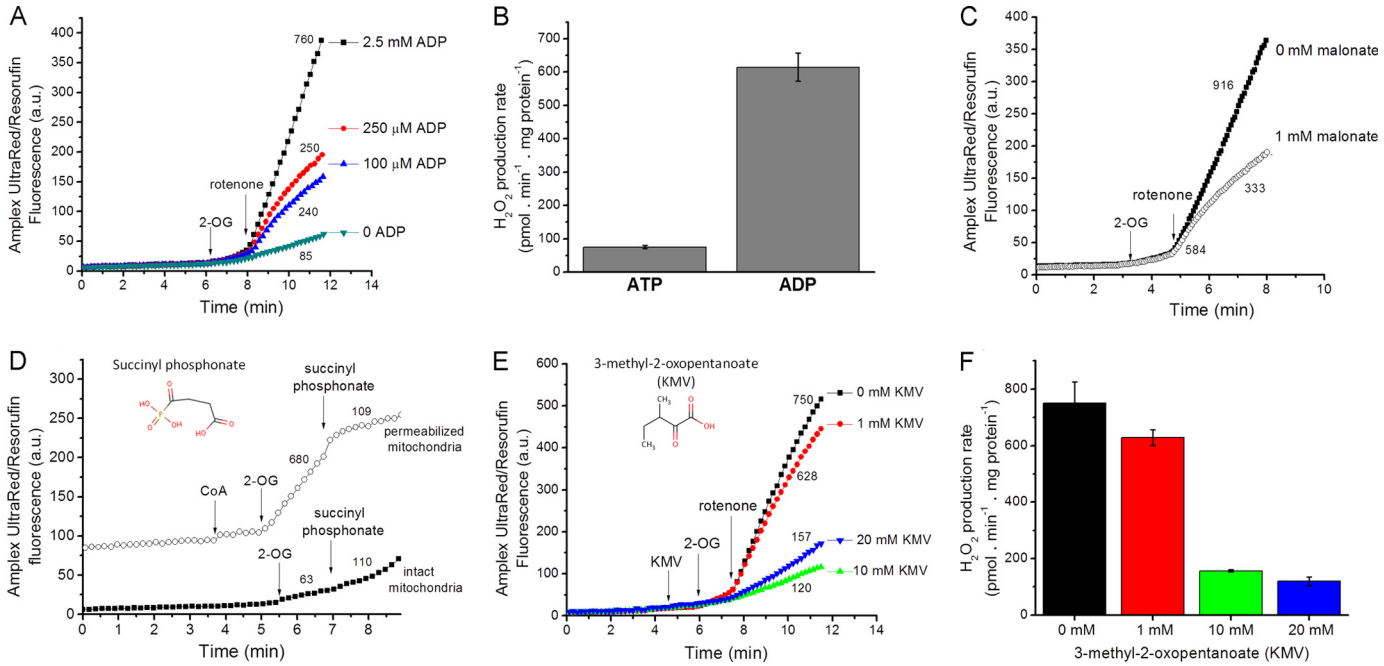

FIGURE 4. **The properties of superoxide/H_2O_2 production by the OGDH complex.** *A*, typical Amplex UltraRed traces indicate that mitochondria suspended in non-phosphorylating medium with 2.5 mM 2-oxoglutarate (*2-OG*) as substrate generated H_2O_2 at relatively low rates in the absence of the positive regulator ADP. Rates were greatly enhanced by the addition of 4 μM rotenone and were dependent on the ADP concentration. *a.u.*, arbitrary units. *B*, mean rates of H_2O_2 production with 2.5 mM 2-oxoglutarate and 4 μM rotenone in the presence of either 2.5 mM ATP or 2.5 mM ADP. Data are the mean ± S.E. ($n = 3$). *C*, Effect of 1 mM malonate on the rates of H_2O_2 production with 2.5 mM 2-oxoglutarate as substrate in the presence of 2.5 mM ADP. *D*, effect of 2 mM succinyl phosphonate on H_2O_2 production rates in intact and alamethicin-permeabilized mitochondria. In the permeabilized mitochondria, 50 μM 2-oxoglutarate was oxidized in the presence of 100 μM CoA. In the intact mitochondria, 50 μM 2-oxoglutarate was oxidized in the presence of 2.5 mM ADP and 4 μM rotenone. *E*, Amplex UltraRed traces show the effect of different concentrations of KMV in the presence of 2.5 mM 2-oxoglutarate and 2.5 mM ADP. *F*, mean rates of H_2O_2 production when OGDH was inhibited by increasing concentrations of 2-methyl-3-oxopentanoate in the presence of 2.5 mM 2-oxoglutarate and 2.5 mM ADP. Data are the means ± S.E. ($n = 3$). *Panels A*, *C*, *D*, and *E* show representative traces; additions are indicated by *arrows*; *numbers* indicate mean rates in pmol of H_2O_2·min^{-1}·mg of protein^{-1} ($n \geq 3$).

depends on thioredoxin and endogenous thiol-disulfide pools. The isolated E1 components of the OGDH and PDH complexes provide still other intermediates to react with oxygen, supposedly generating either H_2O_2 or peracids (58), but occurrence of this side reaction in the native complexes has not been shown.

In our experiments (Fig. 4, *A* and *B*), the observed H_2O_2 production with 2-oxoglutarate in skeletal muscle mitochondria was strongly stimulated by ADP. This probably occurred by two mechanisms, (*a*) lowering the K_d of OGDH for its substrate and (*b*) providing substrate for succinate thiokinase, which regenerates CoA, the substrate of the OGDH complex, and simultaneously removes the potent inhibitor succinyl-CoA (42, 43, 45).

To test whether the observed H_2O_2 production with 2-oxoglutarate was downstream of the OGDH complex, we added malonate, a competitive inhibitor of succinate dehydrogenase (59). However, malonate also inhibits OGDH by acting at the regulatory site responsible for activation by 2-oxoglutarate (60, 61) and may affect 2-oxoglutarate distribution across the mitochondrial inner membrane. Malonate completely inhibits superoxide production by succinate dehydrogenase when succinate concentration is low; inhibition is effectively instantaneous (10). However, with 2-oxoglutarate as substrate, malonate caused a time-dependent inhibition of H_2O_2 production. As shown in Fig. 4*C*, the initial rate (first 10–20 s after rotenone addition) was minimally affected by malonate, but strong inhibition developed over the next few minutes. The time dependence of malonate inhibition, not observed in succinate-dependent H_2O_2 production, suggests that the malonate effect was on the catalytically slow conformational transition involved in substrate-dependent activation of OGDH rather than by competitive inhibition of succinate dehydrogenase.

A good way to test the hypothesis that the OGDH complex is responsible for the majority of the H_2O_2 production observed when 2-oxoglutarate or malate is oxidized would be to inhibit OGDH. Substrate analogs such as succinyl phosphonate are tightly bound and highly specific competitive inhibitors of OGDH (62–65). Unfortunately, succinyl phosphonate was a poor inhibitor of the OGDH complex in mitochondria from rat skeletal muscle compared with those from liver, brain, and kidney (65) (Fig. 4*D*). In alamethicin-permeabilized skeletal muscle mitochondria, succinyl phosphonate strongly inhibited 2-oxoglutarate-dependent production of superoxide/H_2O_2 (Fig. 4*D*), showing that poor transport of succinyl phosphonate explained its weak action in intact rat skeletal muscle mitochondria. Branched-chain 2-oxoacids at millimolar concentrations are known inhibitors of OGDH (66, 67). Fig. 4, *E* and *F*, show that 20 mM KMV inhibited OGDH-dependent H_2O_2 production >80%. However, even at high concentrations 3-methyl-2-oxopentanoate did not fully inhibit all H_2O_2 generation because it was also a substrate for H_2O_2 production by BCKDH (see below).

The production of superoxide/H_2O_2 by NAD^+-linked oxidoreductases is expected to depend on the reduction state of the NADH/NAD^+ pool (11, 19, 20, 26, 27). As discussed above,

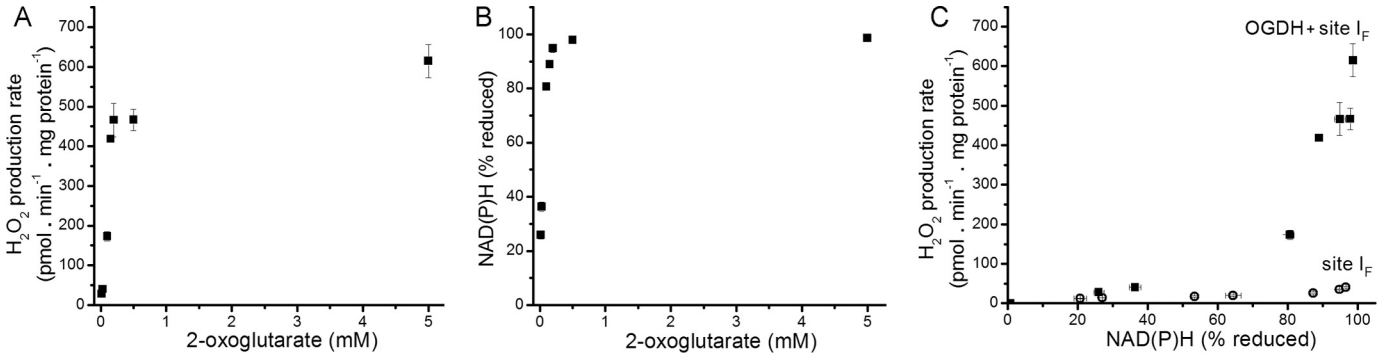

FIGURE 5. **Relationship between the observed rate of H_2O_2 production by the OGDH complex and the reduction state of NAD(P)H.** *A*, dependence of the rate of H_2O_2 production on 2-oxoglutarate concentration in non-phosphorylating medium in the presence of 2.5 mM ADP after the addition of 4 μM rotenone. *B*, dependence of %NAD(P)H reduction on 2-oxoglutarate concentration in non-phosphorylating medium in the presence of 2.5 mM ADP after the addition of rotenone (100% reduction was subsequently established by addition of 5 mM malate). *C*, relationship between the observed rate of H_2O_2 production from the OGDH complex (plus site I_F) and NAD(P)H reduction state (*filled squares*), obtained by combining panels *A* and *B*; *open symbols* are the replotted data for site I_F alone from Fig. 2*D*. Where not visible, *error bars* are contained within the points. Data are the means ± S.E. ($n = 4$).

the reversibility of the complex I-catalyzed reaction implies that NADH/NAD^+ should be close to equilibrium with the superoxide-producing flavin center of complex I. However, the increased matrix NADH/NAD^+ ratio should also increase the rate of superoxide/H_2O_2 production from the OGDH complex because this side reaction is stimulated by the lack of the terminal substrate NAD^+ (19, 50).

Fig. 5, *A* and *B*, shows the dependence of the rate of H_2O_2 production and level of NAD(P)H reduction on 2-oxoglutarate concentration. Combining these data revealed a steep relationship between the H_2O_2 production rate and the reduction state of NAD(P)H as 2-oxoglutarate concentration was varied (*squares*, Fig. 5*C*). Importantly, with malate as substrate (and ATP and aspartate present to inhibit superoxide/H_2O_2 production by the OGDH complex and reveal that from site I_F), there was a different relationship between H_2O_2 production and NAD(P)H reduction (*circles*, Fig. 5*C*). This indicated that (*a*) as NAD(P) became >~80% reduced, the rate of superoxide/H_2O_2 production increased steeply from both the OGDH complex and site I_F, but with very different slopes, and (*b*) the OGDH complex produced superoxide/H_2O_2 much more slowly using electrons from NADH than in the forward reaction from 2-oxoglutarate. As mentioned above, the isolated E3 component of the OGDH complex readily oxidizes NADH and reduces the flavin to generate superoxide/H_2O_2 at relatively high rates (20, 21). However, within the native complex, the 2-oxoglutarate-dependent rate of superoxide/H_2O_2 production is faster than the NADH-dependent rate (68). In our experiments when the NADH pool was reduced in the absence of 2-oxoglutarate (*circles*, Fig. 5*C*), superoxide/H_2O_2 was produced at a much lower rate than with 2-oxoglutarate (*squares*, Fig. 5*C*), indicating that superoxide/H_2O_2 production by the OGDH complex in isolated mitochondria occurred at high rates only in the forward reaction in the presence of 2-oxoglutarate.

Branched-chain 2-Oxoacid Dehydrogenase Complex—The BCKDH complex has strong control over oxidation of the branched-chain amino acids valine, leucine, and isoleucine. These amino acids are converted by specific branched-chain amino acid aminotransferases to their respective branched-chain 2-oxoacids, 3-methyl-2-oxobutanoate (KIV), 4-methyl-2-oxopentanoate (KIC), and KMV, then oxidized by the BCKDH complex to an acyl-CoA, CO_2, and NADH. The complex is phosphorylated and inactivated by BCKDH kinase and dephosphorylated and activated by BCKDH phosphatase, both bound to the E2 core. The kinase belongs to the same family as pyruvate dehydrogenase kinase (69) and is regulated allosterically by inhibitors such as 3-methyl-2-oxobutanoate (KIV) (70) and at the expression level (71).

Fig. 6 shows H_2O_2 production during oxidation of branched-chain 2-oxoacids. The addition of 3-methyl-2-oxopentanoate in the presence of antimycin A stimulated rapid H_2O_2 production (Fig. 6*A*). Under these conditions, several potential sites of superoxide/H_2O_2 production may be active, including complexes I, II, and III. The rate was decreased by myxothiazol (inhibits site Q_o of complex III, *green bar*), indicating that site III_{Qo} was recruited in this condition. It was further decreased by atpenin A5 (*red bar*), an inhibitor of the quinone-binding site of complex II, indicating that 3-methyl-2-oxopentanoate induces superoxide/H_2O_2 production from complex II in the reverse reaction. Both of these effects are driven by reduction of the ubiquinone (Q) pool. A surrogate measure of this is the steady-state reduction level of cytochrome b_{566} (14, 27). Fig. 6*B* shows that the addition of 3-methyl-2-oxopentanoate in the presence of antimycin reduced cytochrome *b* and the Q pool. The addition of rotenone prevented the flow of electrons from 3-methyl-2-oxopentanoate into the Q pool (Fig. 6*B*), eliminating the contributions from site III_{Qo} and site II_F and revealing the maximum rate of superoxide/H_2O_2 production caused by oxidation of 3-methyl-2-oxopentanoate at the level of the NADH isopotential group (Fig. 6*A*, *white* and *blue bars*), *i.e.* by the BCKDH complex plus site I_F.

The rate of superoxide/H_2O_2 production from the BCKDH complex plus site I_F was titrated with KMV (Fig. 6*C*) and 4-methyl-2-oxopentanoate (KIC). The highest rates were obtained with 20 mM 3-methyl-2-oxopentanoate (Fig. 6*D*). We tested whether they were further stimulated by putative inhibitors of BCKDH kinase. However, the addition of leucine or isoleucine (72) or dichloroacetate plus $CaCl_2$ did not increase H_2O_2 production nor did carnitine, which should recycle inhibitory acyl-CoA products (73) and regenerate CoA, a required substrate of BCKDH (Fig. 6*D*).

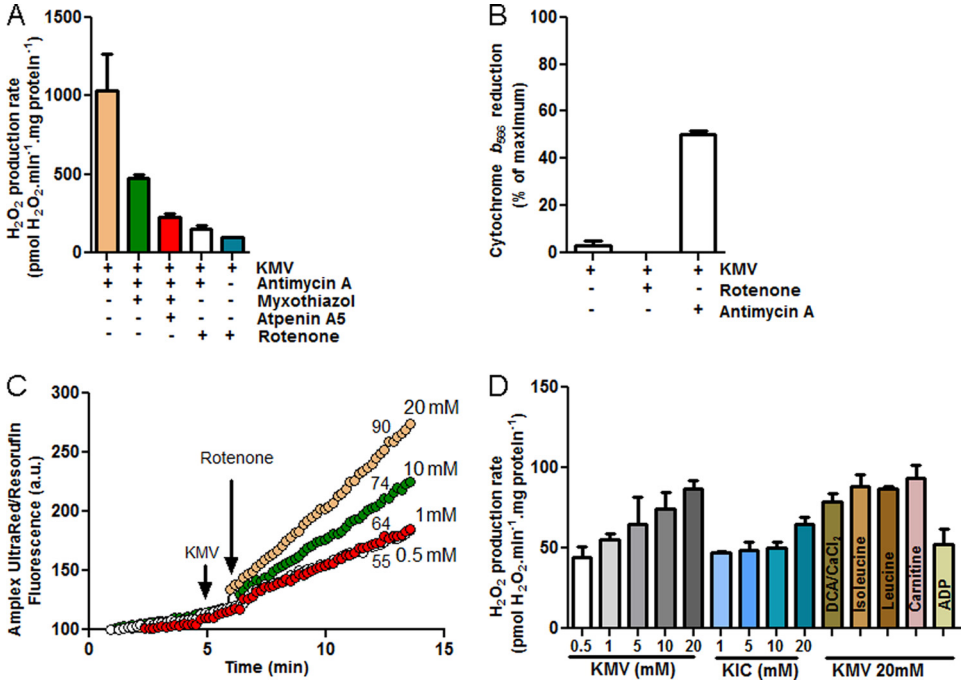

FIGURE 6. **The branched-chain 2-oxoacid dehydrogenase complex produces superoxide/H_2O_2.** *A*, mean rates of H_2O_2 production with 20 mM KMV in non-phosphorylating medium in the presence of 2 μM antimycin A (*beige bar*), 2 μM antimycin A plus 2 μM myxothiazol (*green bar*), 2 μM antimycin A, 2 μM myxothiazol and 2 μM atpenin A5 (*red bar*), 2 μM antimycin A plus 4 μM rotenone (*white bar*), and 4 μM rotenone (*blue bar*). Data are the means ± S.E. ($n = 3$). *B*, cytochrome b_{566} reduction state in non-phosphorylating medium in the presence of 20 mM 3-methyl-2-oxopentanoate plus 4 μM rotenone or plus 2 μM antimycin A. *C*, typical Amplex UltraRed traces indicate that mitochondria suspended in non-phosphorylating medium with different concentrations of 3-methyl-2-oxopentanoate as substrate generated H_2O_2. Rates were greatly enhanced by the addition of 4 μM rotenone. *a.u.*, arbitrary units. *Arrows* indicate additions; *numbers* indicate mean rates in pmol of $H_2O_2 \cdot min^{-1} \cdot$mg of protein^{-1} ($n \geq 3$). *D*, mean rates of H_2O_2 production in non-phosphorylating medium in the presence of the branched-chain 2-oxoacids KMV or KIC at different concentrations and with 20 mM 3-methyl-2-oxopentanoate in the presence of 4 μM rotenone and 450 nM free Ca^{2+} plus 1 mM dichloroacetate (*DCA*), 1 mM isoleucine, 1 mM leucine, 1 mM carnitine, or 2.5 mM ADP. Data are the means ± S.E. ($n = 3$).

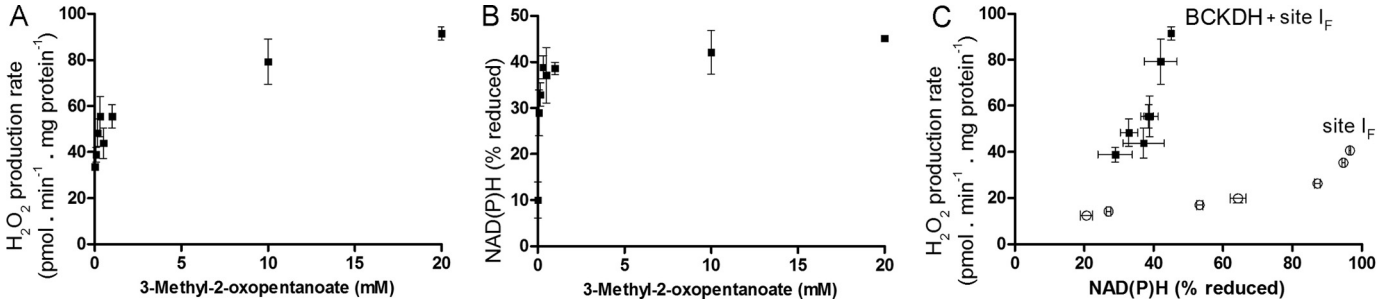

FIGURE 7. **Relationship between the observed rate of H_2O_2 production by the BCKDH complex and the reduction state of NAD(P)H.** *A*, dependence of the rate of H_2O_2 production on KMV concentration in non-phosphorylating medium after the addition of 4 μM rotenone. *B*, dependence of %NAD(P)H reduction on 3-methyl-2-oxopentanoate concentration in non-phosphorylating medium after the addition of rotenone (100% reduction was subsequently established by the addition of 5 mM malate and glutamate). *C*, relationship between the observed rate of H_2O_2 production from the BCKDH complex (plus site I_F) and NAD(P)H reduction state (*filled squares*) obtained by combining panels *A* and *B*; the *open symbols* are the replotted data for site I_F alone from Fig. 2*D*. Where not visible, *error bars* are contained within the points. Data are the means ± S.E. ($n = 4$).

In the presence of oligomycin, ADP inhibited the rate of superoxide/H_2O_2 production with 3-methyl-2-oxopentanoate as substrate (Fig. 6*D*). This is the opposite of its effect with 2-oxoglutarate as substrate (Fig. 4), supporting the hypothesis that the observed H_2O_2 production with 3-methyl-2-oxopentanoate was largely from the BCKDH complex and not a residual activity of the OGDH complex using 3-methyl-2-oxopentanoate as a weak substrate.

Fig. 7, *A* and *B*, show the dependence of the rate of H_2O_2 production and level of NAD(P)H reduction on 3-methyl-2-oxopentanoate concentration. Fig. 7*C* shows that there was a steep relationship between superoxide/H_2O_2 production by the BCKDH complex (plus site I_F), and NAD(P)H level as 3-methyl-2-oxopentanoate was varied. NAD(P) was maximally only 40% reduced, perhaps because of kinetic limitation by the activity of the BCKDH complex, which is inhibited by NADH (73). However, the important observation is that there was a different relationship between H_2O_2 production and NAD(P)H in the presence of 3-methyl-2-oxopentanoate (*squares*, Fig. 7*C*) and in the presence of malate plus aspartate and ATP (*circles*, Fig. 7*C*), indicating that when 3-methyl-2-oxopentanoate is oxidized a different site of superoxide/H_2O_2 production is recruited, most likely the BCKDH complex. Fig. 7*C* shows that the contribution of site I_F to the total observed H_2O_2 production with 20 mM 3-methyl-2-oxopentanoate in these conditions was <20%. It also indicates that the enzyme only produces superoxide/H_2O_2

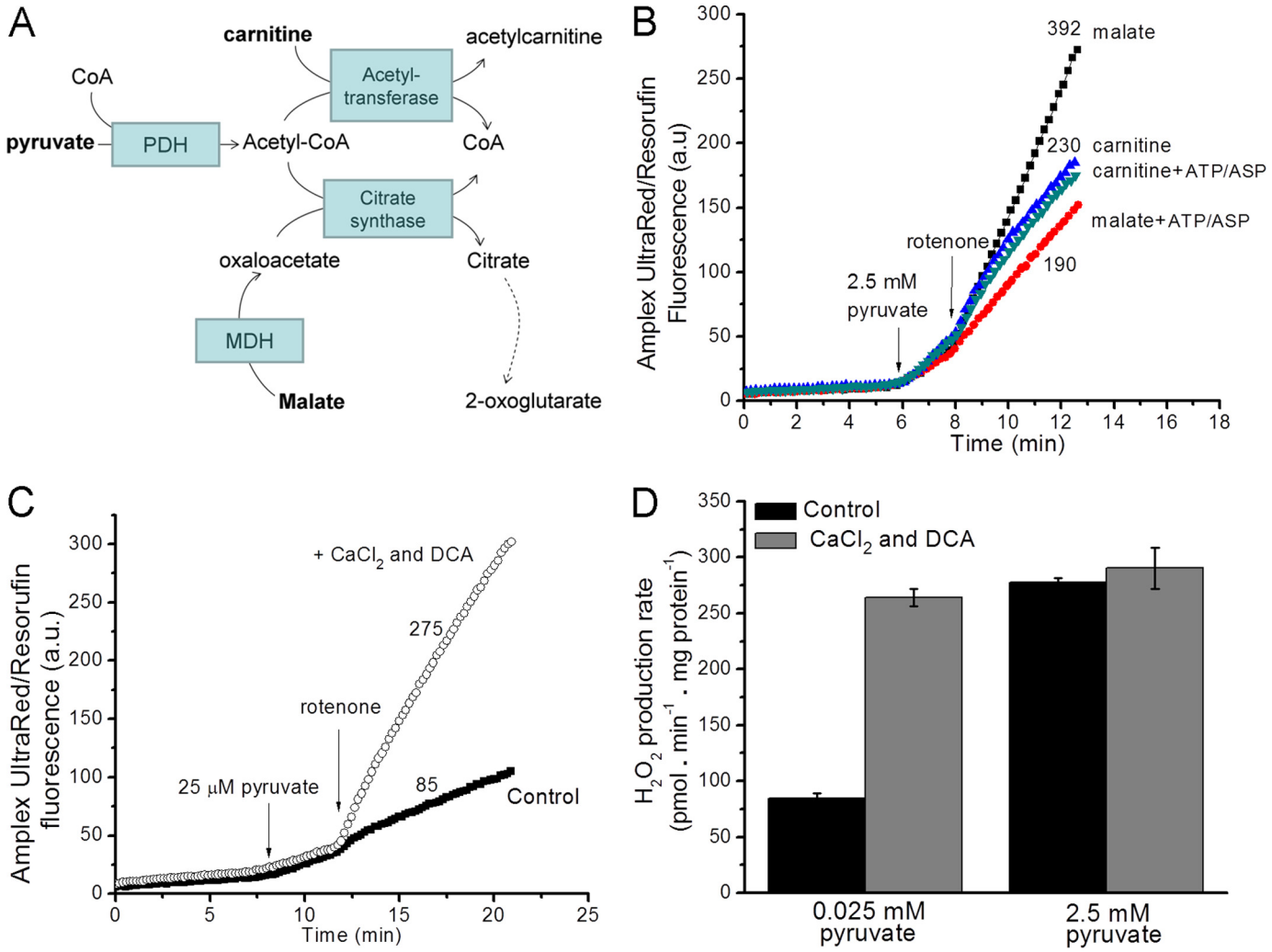

FIGURE 8. **Experimental design for measuring superoxide/H_2O_2 production from the pyruvate dehydrogenase complex.** *A*, carbon flows with pyruvate plus carnitine or pyruvate plus malate as substrates. *MDH*, malate dehydrogenase. *B*, H_2O_2 production in non-phosphorylating medium with 2.5 mM pyruvate plus 5 mM malate or 2.5 mM pyruvate plus 5 mM carnitine as substrate. The contribution from other sites during oxidation of these substrate pairs was assessed by the sensitivity of the rates to 2.5 mM ATP and 1.5 mM aspartate (*ASP*). 4 μM rotenone was added where indicated. *a.u.*, arbitrary units. *C*, Amplex UltraRed traces in non-phosphorylating medium show that at a low pyruvate concentration (25 μM) the rates of H_2O_2 production were low. The presence of 450 nM free Ca^{2+} and 1 mM dichloroacetate (*DCA*) increased the observed rate at low pyruvate concentration. *D*, rates of H_2O_2 production in non-phosphorylating medium at low (25 μM) and high (2.5 mM) pyruvate concentrations in the presence and absence of 450 nM free Ca^{2+} and 1 mM dichloroacetate. Data are the means ± S.E. ($n = 3$). *Panels B* and *C* show representative traces; *numbers* indicate mean rates in pmol of H_2O_2·min^{-1}·mg of $protein^{-1}$ ($n = 3$).

at high rates in the forward reaction (during 3-methyl-2-oxopentanoate oxidation), as the observed rates of H_2O_2 production at the same reduction level of NAD(P)H were always higher in the presence of 3-methyl-2-oxopentanoate.

Pyruvate Dehydrogenase Complex—Mammalian PDH complex is mechanistically similar to the other 2-oxoacid dehydrogenases. Its regulation is similar to that of the BCKDH complex. It is rapidly and reversibly controlled by two mechanisms: end-product inhibition and enzyme phosphorylation/dephosphorylation by specific kinases and phosphatases.

In experiments to assess superoxide/H_2O_2 production by the PDH complex, a primary concern was removal of inhibitory acetyl-CoA, which competes potently with CoA (K_i = 5–10 μM) (74). In isolated mitochondria, acetyl-CoA can be removed by (*a*) the addition of malate to generate oxaloacetate, which will condense with acetyl-CoA to generate citrate through citrate synthase, and (*b*) the addition of carnitine to convert acetyl-CoA to acetylcarnitine, catalyzed by carnitine acetyltransferase (Fig. 8*A*). Removal of acetyl-CoA by either pathway should promote flux through the PDH complex, but the downstream carbon flows will be different. The use of malate as co-substrate with pyruvate promotes Krebs cycle carbon flux, as evident from the decrease in H_2O_2 production when ATP and aspartate were added to suppress that flux (Fig. 8*B*). However, when carnitine was co-substrate with pyruvate, H_2O_2 production was not appreciably affected by ATP and aspartate (Fig. 8*B*). In this system Krebs cycle carbon flows were likely limited as acetylcarnitine was exported from the matrix in exchange for carnitine on the carnitine-acylcarnitine translocase (75, 76).

A second concern was the phosphorylation state of the enzyme (77). Three serines on the α-subunits of E1 may be phosphorylated by four pyruvate dehydrogenase kinases (PDK1–4) (78), inactivating PDH (79). Dephosphorylation is accomplished by two pyruvate dehydrogenase phosphate phosphatases (PDP1 and PDP2). The activities of pyruvate dehydrogenase kinase and dehydrogenase phosphate phosphatase are

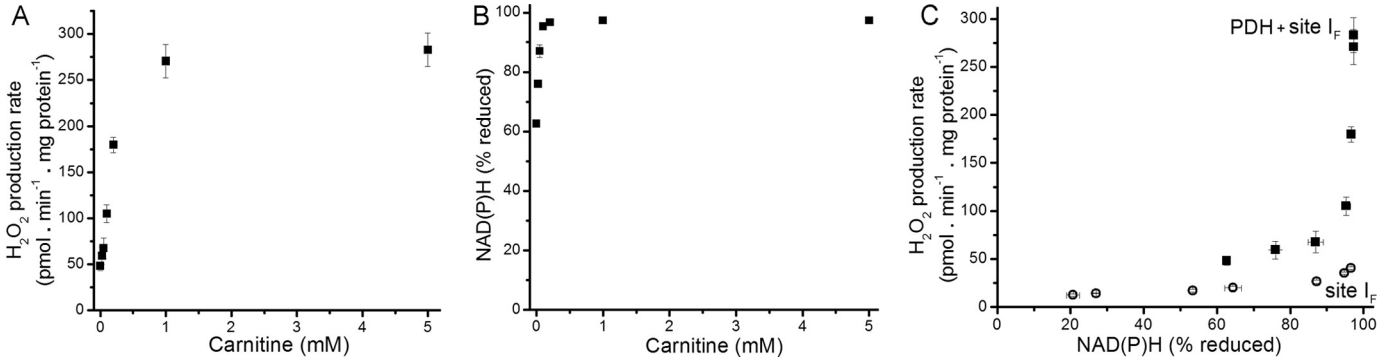

FIGURE 9. **Relationship between the observed rate of H_2O_2 production by the PDH complex and the reduction state of NAD(P)H.** *A*, dependence of the rate of H_2O_2 production on carnitine concentration in non-phosphorylating medium in the presence of 2.5 mM pyruvate and 4 μM rotenone. *B*, dependence of %NAD(P)H reduction on carnitine concentration in non-phosphorylating medium after the addition of rotenone (100% reduction was subsequently established by the addition of 5 mM malate). *C*, relationship between the observed rate of H_2O_2 production from the PDH complex (plus site I_F) and the NAD(P)H reduction state (*filled squares*), obtained by combining *panels A* and *B*; the *open symbols* are the data for site I_F alone from Fig. 2*D*. Where not visible, *error bars* are contained within the points. Data are the means ± S.E. ($n = 3$).

highly regulated. Pyruvate dehydrogenase kinase is inhibited by high concentrations of the E1 substrate pyruvate and activated by acetyl-CoA and NADH, products of both the PDH complex and β-oxidation (80). The non-metabolizable pyruvate analog dichloroacetate inhibits the kinase and thereby activates PDH (81). PDP1, the dominant isoform in muscle, requires Mg^{2+} and is stimulated by Ca^{2+} (82) because PDP1 binding to E2 requires Ca^{2+} (83), and Ca^{2+} decreases the K_m of PDP1 for Mg^{2+} (84).

In skeletal muscle mitochondria, H_2O_2 production after the addition of a low concentration of pyruvate (25 μM) was increased >3-fold by dichloroacetate and $CaCl_2$ (Fig. 8, *C* and *D*). However, at high pyruvate concentrations (2.5 mM), dichloroacetate and $CaCl_2$ did not affect the rate (Fig. 8*D*). These data indicate that at low pyruvate concentrations pyruvate dehydrogenase kinase phosphorylated and inactivated PDH.

Based on these observations, the experimental conditions chosen for assay of superoxide/H_2O_2 production by the PDH complex were a high concentration of pyruvate in the presence of dichloroacetate and $CaCl_2$. The H_2O_2 production rate (Fig. 9*A*) and the steady-state reduction level of NAD(P)H (Fig. 9*B*) were titrated in parallel with carnitine to achieve different steady-state concentrations of inhibitory acetyl-CoA. The data were combined to reveal the relationship between the rate of H_2O_2 production from the PDH complex (plus site I_F) and NAD(P)H reduction state as PDH activity was altered (*squares*, Fig. 9*C*). Similar to the other 2-oxoacid dehydrogenase complexes described above, the rate of superoxide/H_2O_2 production from the PDH complex increased as the NAD(P)H/$NAD(P)^+$ pool was reduced, and PDH was activated by removal of acetyl CoA. As with the OGDH complex, the increase in PDH complex-dependent superoxide/H_2O_2 production at higher NADH/NAD^+ was ascribed to the lack of the terminal substrate NAD^+, as this lack stimulates superoxide production by both PDH and OGDH complexes (19). In contrast, increasing the reduction state of NAD(P) in the absence of pyruvate did not cause rapid superoxide/H_2O_2 production (*circles*, Fig. 9*C*). These observations indicate that superoxide/H_2O_2 production upon oxidation of NADH by the E3 component of the PDH complex was not favored in these intact mitochondria. Thus, superoxide/H_2O_2 production by the PDH complex in isolated mitochondria occurs at high rates only in the forward reaction (during pyruvate oxidation). The E3 subunit is also present in the glycine cleavage system. However, there was no additional H_2O_2 production when glycine was added to rotenone-inhibited mitochondria (<5 pmol of H_2O_2·min^{-1}·mg of protein^{-1}) (not shown).

Effect of Decreasing the Amount of Complex I on Superoxide/H_2O_2 Production—The MWFE subunit of complex I encoded by the X-linked *Ndufa1* gene is essential for complex I assembly (85). Conversion of the evolutionarily conserved serine 55 to alanine (S55A) decreases complex I assembly/activity in mammalian cells (86). Fig. 10*A* confirms that mitochondria from mutant mice carrying the S55A substitution in the MWFE protein had lower levels of complex I.

If the assignment of superoxide/H_2O_2 production in the presence of malate, aspartate, and ATP (*circles*, Fig. 2*D*) to site I_F of complex I is correct, this production should decrease proportionally to the decrease in complex I in mitochondria from the mutant mice; Fig. 10*B* shows that this was indeed the case. Conversely, if we have correctly assigned superoxide/H_2O_2 production with 2-oxoacid substrates (Figs. 5*C*, 7*C*, and 9*C*) to the appropriate 2-oxoacid dehydrogenase complex, this production should not be affected by a decrease in complex I; Fig. 10, *C*, *D*, and *E*, shows that no decrease in H_2O_2 production was observed with these substrates in the mutant (from Fig. 10*B* the contribution of site I_F would be only 0.5, 9, and 2% respectively, too small to register). Similarly, we assign superoxide/H_2O_2 production with malate as substrate (*squares*, Fig. 2*D*) to the OGDH complex plus site I_F; Fig. 10*F* shows that no decrease was observed in the mutant (the contribution of site I_F would be only 6%). These observations strongly support our assignments of superoxide/H_2O_2 production to the specific sites mentioned.

Superoxide production from site I_Q of complex I should also decrease proportionally to the decrease in complex I. We did not observe the predicted decrease when site I_Q was driven by succinate oxidation, but this can be explained by measured compensatory increases in the amount of complex II and the magnitude of the proton-motive force during succinate oxidation (not shown).

Mice lacking apoptosis-inducing factor also have compromised complex I assembly, and superoxide/H_2O_2 generation

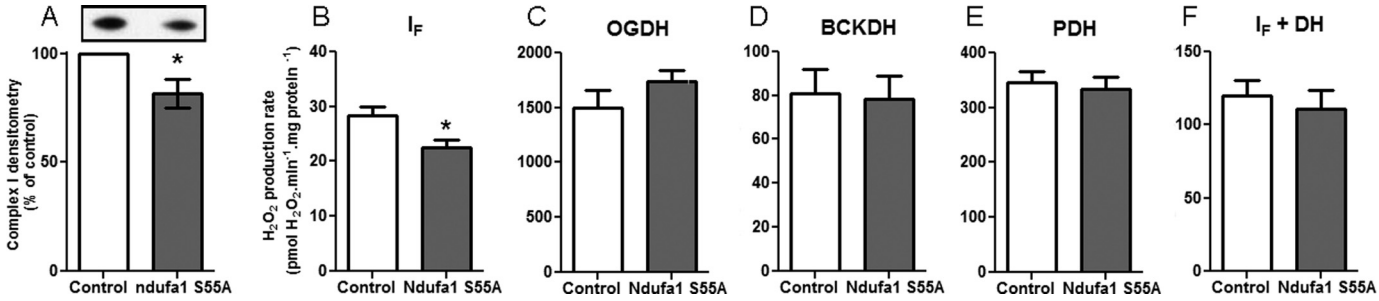

FIGURE 10. **Superoxide/H_2O_2 production by mitochondria from complex I-deficient *Ndufa1*$^{S55A/Y}$ mice.** *A*, densitometry of Western blots of mitochondria from wild type and mutant mice probed for the 75-kDa NDUFS1 subunit of complex I (*inset*, representative Western blot. *Left*, control; *right*, *Ndufa*$^{S55A/Y}$). *B–F*, superoxide/H_2O_2 generation in non-phosphorylating medium after the addition of 4 μM rotenone by mitochondria from control (*white bars*) or complex I deficient (*Ndufa*$^{S55A/Y}$) mice (*gray bars*) in the presence of 5 mM malate, 2.5 mM ATP, and 1.5 mM aspartate (*B*), 2.5 mM 2-oxoglutarate and 2.5 mM ADP (*C*), 20 mM 3-methyl-2-oxopentanoate (*D*), 2.5 mM pyruvate and 5 mM carnitine (*E*), and 5 mM malate (*F*). *DH*, NADH dehydrogenases. Data in *A* are expressed as % of paired control from five independent paired skeletal muscle mitochondrial preparations; *error bars* indicate 95% confidence limits; *, $p < 0.05$ by 95% confidence interval. Data in *B–F* are the means ± S.E. ($n = 5$); *, $p < 0.05$ by Student's *t* test.

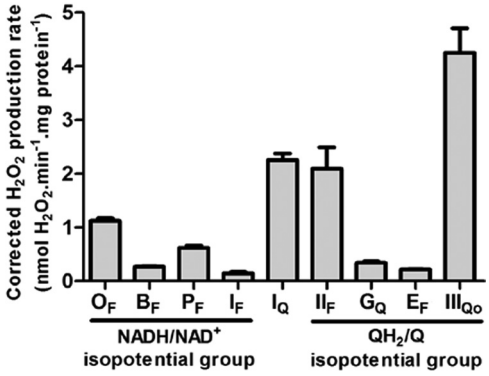

FIGURE 11. **Maximum rates of superoxide/H_2O_2 production from characterized sites of the mitochondrial respiratory chain.** The components of the NADH/NAD$^+$ isopotential group are: O_F, flavin site of 2-oxoglutarate dehydrogenase; B_F, flavin site of branched-chain 2-oxoacid dehydrogenase; P_F, flavin site of pyruvate dehydrogenase; I_F, flavin site of complex I. The ubiquinone binding site of complex I (site I_Q) is between isopotential groups. The components of the QH_2/Q isopotential group are: II_F, flavin site of complex II; G_Q, quinone site of mitochondrial glycerol-3-phosphate dehydrogenase; E_F, flavin site of the electron transferring flavoprotein/ETF:ubiquinone oxidoreductase system; III_{Qo}, Q_o binding site of complex III. All data were mathematically corrected for matrix peroxidase activity using the 1-chloro-2,4-dinitrobenzene correction described under "Experimental Procedures." Data for O_F, B_F, P_F, and I_F are from Figs. 5*C*, 7*C*, 9*C*, and 2*D* (plus aspartate/ATP); other sites are replotted from (16). The maximum rates from O_F, B_F, and P_F were corrected by subtracting the rate from site I_F at the same NAD(P)H reduction level. Data are the means ± S.E. ($n \geq 3$).

from site I_Q was decreased in brain mitochondria from these mice (87). However, H_2O_2 production driven by glutamate plus malate in the presence of rotenone was not, suggesting that "the major source of superoxide/H_2O_2 in this model may lie outside complex I" (see Ref. 87). Our results (Fig. 10) confirm these observations in a different model and support the conclusion that the OGHD complex is the major site of superoxide/H_2O_2 generation with glutamate plus malate as substrate in the presence of rotenone.

Maximum Capacities of Specific Sites of Superoxide/H_2O_2 Production in Intact Skeletal Muscle Mitochondria—Fig. 11 puts the *in situ* capacities of the superoxide/H_2O_2 producing sites of the NADH/NAD$^+$ isopotential group in context. It shows the maximum rates from the OGDH, BCKDH, and PDH complexes, site I_F, site I_Q, site II_F, mitochondrial glycerol-3-phosphate dehydrogenase, electron transferring flavoprotein/ETF:ubiquinone oxidoreductase, and site III_{Qo} (all after correction for matrix peroxidase activity using the correction described under "Experimental Procedures"). For this correction, we assumed that 100% of the superoxide/H_2O_2 from site I_F and the 2-oxoacid dehydrogenase complexes was superoxide or H_2O_2 produced to the matrix, as the rates were insensitive to the addition of exogenous superoxide dismutase (not shown). Of the nine sites examined, site I_F had the lowest maximum capacity in skeletal muscle mitochondria. The maximum rate of superoxide/H_2O_2 production by the OGDH complex was ~8 times higher than the maximum rate of superoxide production from site I_F; the maximum rate from the PDH complex was more than four times higher, and the maximum rate from the BCKDH complex was almost twice the rate from site I_F. Although not as high as the maximal rates from the producers with the greatest capacities, I_Q, II_F, and III_{Qo}, the rates from the OGDH, PDH, and BCKDH complexes were a much higher proportion of the rate from the NADH/NAD$^+$ isopotential group in the presence of rotenone than we and many others originally envisaged (1–9, 25–27).

Conclusions—When electron transport through complex I is inhibited by rotenone, the NADH/NAD$^+$ pool becomes reduced, and the enzymes in the isopotential group around this pool, specifically the OGDH, BCKDH, and PDH complexes and site I_F, generate more superoxide and/or H_2O_2. The contributions of the different sites depend on the conditions. Because site I_F is close to equilibrium with the matrix NADH/NAD$^+$ pool, its rate of superoxide production is a simple function of the redox state of the NADH/NAD$^+$, described by the lower set of points in Fig. 2*D*.

Although they tend to become more reduced and generate superoxide/H_2O_2 at higher rates in the presence of their specific substrates when NADH is high, the redox centers that produce superoxide/H_2O_2 in the OGDH, BCKDH, and PDH complexes are not in equilibrium with the NADH/NAD$^+$ pool. This is clear from Figs. 5*C*, 7*C*, and 9*C*, which show that the OGDH, BCKDH, and PDH complexes do not generate superoxide/H_2O_2 at high rates in the absence of 2-oxoglutarate, 3-methyl-2-oxopentanoate, or pyruvate, respectively (lower sets of points) even when NADH/NAD$^+$ is high. Therefore, superoxide/H_2O_2 production at the OGDH (or BCKDH or PDH) complex does not have a unique relationship to NADH/NAD$^+$; instead it also depends on the concentration of 2-oxo-

glutarate (or branched chain 2-oxoacid or pyruvate) and on the activation state of the enzyme.

Under optimal conditions for each system in mitochondria isolated from rat skeletal muscle, the OGDH complex can produce superoxide/H_2O_2 at about eight times the rate from site I_F (Fig. 5*C*), the PDH complex can produce superoxide/H_2O_2 at about four times the rate from site I_F (Fig. 9*C*), and the BCKDH complex can produce superoxide/H_2O_2 at almost twice the rate from site I_F (Fig. 7*C*). Depending on the substrates present and the conditions, the dominant sites of superoxide/H_2O_2 production at the level of the NADH/NAD^+ isopotential pool may be the OGDH and PDH complexes, but in the past their superoxide/H_2O_2 production may often have been misattributed to complex I.

REFERENCES

1. Hansford, R. G., Hogue, B. A., and Mildaziene, V. (1997) Dependence of H_2O_2 formation by rat heart mitochondria on substrate availability and donor age. *J. Bioenerg. Biomembr.* **29,** 89–95
2. Barja, G., and Herrero, A. (1998) Localization at complex I and mechanism of the higher free radical production of brain nonsynaptic mitochondria in the short-lived rat than in the longevous pigeon. *J. Bioenerg. Biomembr.* **30,** 235–243
3. Kushnareva, Y., Murphy, A. N., and Andreyev, A. (2002) Complex I-mediated reactive oxygen species generation. Modulation by cytochrome *c* and $NAD(P)^+$ oxidation-reduction state. *Biochem. J.* **368,** 545–553
4. St-Pierre, J., Buckingham, J. A., Roebuck, S. J., and Brand, M. D. (2002) Topology of superoxide production from different sites in the mitochondrial electron transport chain. *J. Biol. Chem.* **277,** 44784–44790
5. Andreyev, A. Y., Kushnareva, Y. E., and Starkov, A. A. (2005) Mitochondrial metabolism of reactive oxygen species. *Biochemistry* **70,** 200–214
6. Murphy, M. P. (2009) How mitochondria produce reactive oxygen species. *Biochem. J.* **417,** 1–13
7. Brand, M. D. (2010) The sites and topology of mitochondrial superoxide production. *Exp. Gerontol.* **45,** 466–472
8. Quinlan, C. L., Treberg, J. R., and Brand, M. D. (2011) Mechanisms of mitochondrial free radical production and their relationship to the aging process. In *Handbook of the Biology of Aging* (Masoro, E. J., and Austad, S. N., eds) 7th Ed., pp. 47–61, Elsevier, Amsterdam
9. Quinlan, C. L., Perevoschikova, I. V., Goncalves, R. L., Hey-Mogensen, M., and Brand, M. D. (2013) The determination and analysis of site-specific rates of mitochondrial reactive oxygen species production. *Methods Enzymol.* **526,** 189–217
10. Quinlan, C. L., Orr, A. L., Perevoshchikova, I. V., Treberg, J. R., Ackrell, B. A., and Brand, M. D. (2012) Mitochondrial complex II can generate reactive oxygen species at high rates in both the forward and reverse reactions. *J. Biol. Chem.* **287,** 27255–27264
11. Treberg, J. R., Quinlan, C. L., and Brand, M. D. (2011) Evidence for two sites of superoxide production by mitochondrial NADH-ubiquinone oxidoreductase (complex I). *J. Biol. Chem.* **286,** 27103–27110
12. Kramer, D. M., Roberts, A. G., Muller, F., Cape, J., and Bowman, M. K. (2004) Q-cycle bypass reactions at the Qo site of the cytochrome bc_1 (and related) complexes. *Methods Enzymol.* **382,** 21–45
13. Muller, F. L., Roberts, A. G., Bowman, M. K., and Kramer, D. M. (2003) Architecture of the Qo site of the cytochrome bc_1 complex probed by superoxide production. *Biochemistry* **42,** 6493–6499
14. Quinlan, C. L., Gerencser, A. A., Treberg, J. R., and Brand, M. D. (2011) The mechanism of superoxide production by the antimycin-inhibited mitochondrial Q-cycle. *J. Biol. Chem.* **286,** 31361–31372
15. Orr, A. L., Quinlan, C. L., Perevoshchikova, I. V., and Brand, M. D. (2012) A refined analysis of superoxide production by mitochondrial *sn*-glycerol-3-phosphate dehydrogenase. *J. Biol. Chem.* **287,** 42921–42935
16. Perevoshchikova, I. V., Quinlan, C. L., Orr, A. L., Gerencser, A. A., and Brand, M. D. (2013) Sites of superoxide and hydrogen peroxide production during fatty acid oxidation in rat skeletal muscle mitochondria. *Free Radic. Biol. Med.* **61,** 298–309
17. Forman, H. J., and Kennedy, J. (1975) Superoxide production and electron transport in mitochondrial oxidation of dihydroorotic acid. *J. Biol. Chem.* **250,** 4322–4326
18. Kareyeva, A. V., Grivennikova, V. G., Cecchini, G., and Vinogradov, A. D. (2011) Molecular identification of the enzyme responsible for the mitochondrial NADH-supported ammonium-dependent hydrogen peroxide production. *FEBS Lett.* **585,** 385–389
19. Bunik, V. I., and Sievers, C. (2002) Inactivation of the 2-oxo acid dehydrogenase complexes upon generation of intrinsic radical species. *Eur. J. Biochem.* **269,** 5004–5015
20. Starkov, A. A., Fiskum, G., Chinopoulos, C., Lorenzo, B. J., Browne, S. E., Patel, M. S., and Beal, M. F. (2004) Mitochondrial α-ketoglutarate dehydrogenase complex generates reactive oxygen species. *J. Neurosci.* **24,** 7779–7788
21. Tretter, L., and Adam-Vizi, V. (2004) Generation of reactive oxygen species in the reaction catalyzed by α-ketoglutarate dehydrogenase. *J. Neurosci.* **24,** 7771–7778
22. Ambrus, A., and Adam-Vizi, V. (2013) Molecular dynamics study of the structural basis of dysfunction and the modulation of reactive oxygen species generation by pathogenic mutants of human dihydrolipoamide dehydrogenase. *Arch. Biochem. Biophys.* **538,** 145–155
23. Fisher-Wellman, K. H., Gilliam, L. A., Lin, C. T., Cathey, B. L., Lark, D. S., and Darrell Neufer, P. (2013) Mitochondrial glutathione depletion reveals a novel role for the pyruvate dehydrogenase complex as a key HO-emitting source under conditions of nutrient overload. *Free Radic. Biol. Med.* **65,** 1201–1208
24. White, T. A., Krishnan, N., Becker, D. F., and Tanner, J. J. (2007) Structure and kinetics of monofunctional proline dehydrogenase from *Thermus thermophilus*. *J. Biol. Chem.* **282,** 14316–14327
25. Brand, M. D., Orr, A. L., Perevoschikova, I. V., and Quinlan, C. L. (2013) The role of mitochondrial function and cellular bioenergetics in aging and disease. *Br. J. Dermatol.* **169,** 1–8
26. Quinlan, C. L., Perevoshchikova, I. V., Hey-Mogensen, M., Orr, A. L., and Brand, M. D. (2013) Sites of reactive oxygen species generation by mitochondria oxidizing different substrates. *Redox Biol.* **1,** 304–312
27. Quinlan, C. L., Treberg, J. R., Perevoshchikova, I. V., Orr, A. L., and Brand, M. D. (2012) Native rates of superoxide production from multiple sites in isolated mitochondria measured using endogenous reporters. *Free Radic. Biol. Med.* **53,** 1807–1817
28. Massey, V. (1994) Activation of molecular oxygen by flavins and flavoproteins. *J. Biol. Chem.* **269,** 22459–22462
29. Zhang, L., Yu, L., and Yu, C. A. (1998) Generation of superoxide anion by succinate-cytochrome *c* reductase from bovine heart mitochondria. *J. Biol. Chem.* **273,** 33972–33976
30. Kussmaul, L., and Hirst, J. (2006) The mechanism of superoxide production by NADH:ubiquinone oxidoreductase (complex I) from bovine heart mitochondria. *Proc. Natl. Acad. Sci. U.S.A.* **103,** 7607–7612
31. Affourtit, C., Quinlan, C. L., and Brand, M. D. (2012) Measurement of proton leak and electron leak in isolated mitochondria. *Methods Mol. Biol.* **810,** 165–182
32. Treberg, J. R., Quinlan, C. L., and Brand, M. D. (2010) Hydrogen peroxide efflux from muscle mitochondria underestimates matrix superoxide production. A correction using glutathione depletion. *FEBS J.* **277,** 2766–2778
33. Grivennikova, V. G., Kapustin, A. N., and Vinogradov, A. D. (2001) Catalytic activity of NADH-ubiquinone oxidoreductase (complex I) in intact mitochondria. Evidence for the slow active/inactive transition. *J. Biol. Chem.* **276,** 9038–9044
34. Nicholls, D. G., and Ferguson, S. J. (2013) *Bioenergetics 4*, p. 107, Academic Press Inc., London
35. Chan, P. C., and Bielski, B. H. (1974) Enzyme-catalyzed free radical reactions with nicotinamide adenine nucleotides. II. Lactate dehydrogenase-catalyzed oxidation of reduced nicotinamide adenine dinucleotide by superoxide radicals generated by xanthine oxidase. *J. Biol. Chem.* **249,** 1317–1319
36. Lambert, A. J., and Brand, M. D. (2004) Inhibitors of the quinone-binding site allow rapid superoxide production from mitochondrial NADH:

ubiquinone oxidoreductase (complex I). *J. Biol. Chem.* **279,** 39414–39420
37. Lambert, A. J., and Brand, M. D. (2004) Superoxide production by NADH: ubiquinone oxidoreductase (complex I) depends on the pH gradient across the mitochondrial inner membrane. *Biochem. J.* **382,** 511–517
38. Lambert, A. J., Buckingham, J. A., Boysen, H. M., and Brand, M. D. (2008) Diphenyleneiodonium acutely inhibits reactive oxygen species production by mitochondrial complex I during reverse, but not forward electron transport. *Biochim. Biophys. Acta* **1777,** 397–403
39. Lambert, A. J., Buckingham, J. A., and Brand, M. D. (2008) Dissociation of superoxide production by mitochondrial complex I from NAD(P)H redox state. *FEBS Lett.* **582,** 1711–1714
40. Orr, A. L., Ashok, D., Sarantos, M. R., Shi, T., Hughes, R. E., and Brand, M. D. (2013) Inhibitors of ROS production by the ubiquinone-binding site of mitochondrial complex I identified by chemical screening. *Free Radic. Biol. Med.* **65,** 1047–1059
41. Pryde, K. R., and Hirst, J. (2011) Superoxide is produced by the reduced flavin in mitochondrial complex I. A single, unified mechanism that applies during both forward and reverse electron transfer. *J. Biol. Chem.* **286,** 18056–18065
42. Qi, F., Pradhan, R. K., Dash, R. K., and Beard, D. A. (2011) Detailed kinetics and regulation of mammalian 2-oxoglutarate dehydrogenase. *BMC Biochem.* **12,** 53
43. Bunik, V., Raddatz, G., and Strumilo, S. (2013) Translating enzymology into metabolic regulation. The case of the 2-oxoglutarate dehydrogenase multienzyme complex. *Curr. Chem. Biol.* **7,** 74–93
44. Lambeth, D. O., Tews, K. N., Adkins, S., Frohlich, D., and Milavetz, B. I. (2004) Expression of two succinyl-CoA synthetases with different nucleotide specificities in mammalian tissues. *J. Biol. Chem.* **279,** 36621–36624
45. Garland, P. B. (1964) Some kinetic properties of pig-heart oxoglutarate dehydrogenase that provide a basis for metabolic control of the enzyme activity and also a stoicheiometric assay for coenzyme A in tissue extracts. *Biochem. J.* **92,** 10C–12C
46. Kareyeva, A. V., Grivennikova, V. G., and Vinogradov, A. D. (2012) Mitochondrial hydrogen peroxide production as determined by the pyridine nucleotide pool and its redox state. *Biochim. Biophys. Acta* **1817,** 1879–1885
47. Grivennikova, V. G., and Vinogradov, A. D. (2013) Partitioning of superoxide and hydrogen peroxide production by mitochondrial respiratory complex I. *Biochim. Biophys. Acta* **1827,** 446–454
48. Izard, T., Aevarsson, A., Allen, M. D., Westphal, A. H., Perham, R. N., de Kok, A., and Hol, W. G. (1999) Principles of quasi-equivalence and Euclidean geometry govern the assembly of cubic and dodecahedral cores of pyruvate dehydrogenase complexes. *Proc. Natl. Acad. Sci. U.S.A.* **96,** 1240–1245
49. Perham, R. N. (1991) Domains, motifs, and linkers in 2-oxo acid dehydrogenase multienzyme complexes. A paradigm in the design of a multifunctional protein. *Biochemistry* **30,** 8501–8512
50. Bunik, V. I. (2003) 2-Oxo acid dehydrogenase complexes in redox regulation. *Eur. J. Biochem.* **270,** 1036–1042
51. Zündorf, G., Kahlert, S., Bunik, V. I., and Reiser, G. (2009) α-Ketoglutarate dehydrogenase contributes to production of reactive oxygen species in glutamate-stimulated hippocampal neurons in situ. *Neuroscience* **158,** 610–616
52. Tretter, L., and Adam-Vizi, V. (2005) α-Ketoglutarate dehydrogenase. A target and generator of oxidative stress. *Philos. Trans. R. Soc. Lond. B Biol. Sci.* **360,** 2335–2345
53. Massey, V., Müller, F., Feldberg, R., Schuman, M., Sullivan, P. A., Howell, L. G., Mayhew, S. G., Matthews, R. G., and Foust, G. P. (1969) The reactivity of flavoproteins with sulfite. Possible relevance to the problem of oxygen reactivity. *J. Biol. Chem.* **244,** 3999–4006
54. Massey, V., Strickland, S., Mayhew, S. G., Howell, L. G., Engel, P. C., Matthews, R. G., Schuman, M., and Sullivan, P. A. (1969) The production of superoxide anion radicals in the reaction of reduced flavins and flavoproteins with molecular oxygen. *Biochem. Biophys. Res. Commun.* **36,** 891–897
55. Kunz, W. S., and Gellerich, F. N. (1993) Quantification of the content of fluorescent flavoproteins in mitochondria from liver, kidney cortex, skeletal muscle, and brain. *Biochem. Med. Metab. Biol.* **50,** 103–110
56. Kunz, W. S., and Kunz, W. (1985) Contribution of different enzymes to flavoprotein fluorescence of isolated rat liver mitochondria. *Biochim. Biophys. Acta* **841,** 237–246
57. Asmus, K. D. (1990) Sulfur-centered free radicals. *Methods Enzymol.* **186,** 168–180
58. Bunik, V. I., Schloss, J. V., Pinto, J. T., Dudareva, N. D., and Cooper, A. J. L. (2011) A survey of oxidative paracatalytic reactions catalyzed by enzymes that generate carbanionic intermediates. Implications for ROS production, cancer etiology, and neurodegenerative diseases. *Adv. Enzymol. Rel. Areas Mol. Biol.* **77,** 305–358
59. Gutman, M., Kearney, E. B., and Singer, T. P. (1971) Control of succinate dehydrogenase in mitochondria. *Biochemistry* **10,** 4763–4770
60. Bunik, V. I., Romash, O. G., and Gomazkova, V. S. (1991) Effect of α-ketoglutarate and its structural analogues on hysteretic properties of α-ketoglutarate dehydrogenase. *FEBS Lett.* **278,** 147–150
61. Bunik, V., Westphal, A. H., and de Kok, A. (2000) Kinetic properties of the 2-oxoglutarate dehydrogenase complex from *Azotobacter vinelandii*. Evidence for the formation of a precatalytic complex with 2-oxoglutarate. *Eur. J. Biochem.* **267,** 3583–3591
62. Bunik, V. I., Biryukov, A. I., and Zhukov, YuN (1992) Inhibition of pigeon breast muscle α-ketoglutarate dehydrogenase by phosphonate analogues of α-ketoglutarate. *FEBS Lett.* **303,** 197–201
63. Biryukov, A. I., Bunik, V. I., Zhukov, Y. N., Khurs, E. N., and Khomutov, R. M. (1996) Succinyl phosphonate inhibits α-ketoglutarate oxidative decarboxylation, catalyzed by α-ketoglutarate dehydrogenase complexes from *E. coli* and pigeon breast muscle. *FEBS Lett.* **382,** 167–170
64. Bunik, V. I., Denton, T. T., Xu, H., Thompson, C. M., Cooper, A. J., and Gibson, G. E. (2005) Phosphonate analogues of α-ketoglutarate inhibit the activity of the α-ketoglutarate dehydrogenase complex isolated from brain and in cultured cells. *Biochemistry* **44,** 10552–10561
65. Cheshchevic, V., Janssen, A. J. M., Dremza, I. K., Zavodnik, I. B., and Bunik, V. I. (2010) The OGDHC-exerted control of mitochondrial respiration is increased under energy demand. In *Mitochondrial Physiology. The Many Functions of the Organism in Our Cells.* (Renner-Sattler, K., and Gnaiger, E., eds.) pp 76–77, Steiger Druck GmbH, Axams, Austria
66. Patel, M. S. (1974) Inhibition by the branched-chain 2-oxo acids of the 2-oxoglutarate dehydrogenase complex in developing rat and human brain. *Biochem. J.* **144,** 91–97
67. Shestopalov, A. I., and Kristal, B. S. (2007) Branched chain keto-acids exert biphasic effects on α-ketoglutarate-stimulated respiration in intact rat liver mitochondria. *Neurochem. Res.* **32,** 947–951
68. Bunik, V. I., and Fernie, A. R. (2009) Metabolic control exerted by the 2-oxoglutarate dehydrogenase reaction. A cross-kingdom comparison of the crossroad between energy production and nitrogen assimilation. *Biochem. J.* **422,** 405–421
69. Harris, R. A., Popov, K. M., Zhao, Y., Kedishvili, N. Y., Shimomura, Y., and Crabb, D. W. (1995) A new family of protein kinases. The mitochondrial protein kinases. *Adv. Enzyme Regul.* **35,** 147–162
70. Paxton, R., and Harris, R. A. (1984) Regulation of branched-chain α-keto-acid dehydrogenase kinase. *Arch. Biochem. Biophys.* **231,** 48–57
71. Harris, R. A., Joshi, M., and Jeoung, N. H. (2004) Mechanisms responsible for regulation of branched-chain amino acid catabolism. *Biochem. Biophys. Res. Commun.* **313,** 391–396
72. Parker, P. J., and Randle, P. J. (1978) Branched chain 2-oxo-acid dehydrogenase complex of rat liver. *FEBS Lett.* **90,** 183–186
73. Parker, P. J., and Randle, P. J. (1978) Partial purification and properties of branched-chain 2-oxo acid dehydrogenase of ox liver. *Biochem. J.* **171,** 751–757
74. Wieland, O. H. (1983) The mammalian pyruvate dehydrogenase complex. Structure and regulation. *Rev. Physiol. Biochem. Pharmacol.* **96,** 123–170
75. Ramsay, R. R., and Tubbs, P. K. (1975) The mechanism of fatty acid uptake by heart mitochondria. An acylcarnitine-carnitine exchange. *FEBS Lett.* **54,** 21–25
76. Pande, S. V., and Parvin, R. (1976) Characterization of carnitine acylcarnitine translocase system of heart mitochondria. *J. Biol. Chem.* **251,** 6683–6691
77. Roche, T. E., Hiromasa, Y., Turkan, A., Gong, X., Peng, T., Yan, X., Kasten, S. A., Bao, H., and Dong, J. (2003) Essential roles of lipoyl domains in the

activated function and control of pyruvate dehydrogenase kinases and phosphatase isoform 1. *Eur. J. Biochem.* **270,** 1050–1056
78. Yeaman, S. J., Hutcheson, E. T., Roche, T. E., Pettit, F. H., Brown, J. R., Reed, L. J., Watson, D. C., and Dixon, G. H. (1978) Sites of phosphorylation on pyruvate dehydrogenase from bovine kidney and heart. *Biochemistry* **17,** 2364–2370
79. Linn, T. C., Pettit, F. H., and Reed, L. J. (1969) α-Keto acid dehydrogenase complexes. X. Regulation of the activity of the pyruvate dehydrogenase complex from beef kidney mitochondria by phosphorylation and dephosphorylation. *Proc. Natl. Acad. Sci. U.S.A.* **62,** 234–241
80. Kerbey, A. L., Randle, P. J., Cooper, R. H., Whitehouse, S., Pask, H. T., and Denton, R. M. (1976) Regulation of pyruvate dehydrogenase in rat heart. Mechanism of regulation of proportions of dephosphorylated and phosphorylated enzyme by oxidation of fatty acids and ketone bodies and of effects of diabetes. Role of coenzyme A, acetyl-coenzyme A, and reduced and oxidized nicotinamide-adenine dinucleotide. *Biochem. J.* **154,** 327–348
81. Stacpoole, P. W. (1989) The pharmacology of dichloroacetate. *Metabolism* **38,** 1124–1144
82. Huang, B., Gudi, R., Wu, P., Harris, R. A., Hamilton, J., and Popov, K. M. (1998) Isoenzymes of pyruvate dehydrogenase phosphatase. DNA-derived amino acid sequences, expression, and regulation. *J. Biol. Chem.* **273,** 17680–17688
83. Pettit, F. H., Roche, T. E., and Reed, L. J. (1972) Function of calcium ions in pyruvate dehydrogenase phosphatase activity. *Biochem. Biophys. Res. Commun.* **49,** 563–571
84. Thomas, A. P., Diggle, T. A., and Denton, R. M. (1986) Sensitivity of pyruvate dehydrogenase phosphate phosphatase to magnesium ions. Similar effects of spermine and insulin. *Biochem. J.* **238,** 83–91
85. Yadava, N., Houchens, T., Potluri, P., and Scheffler, I. E. (2004) Development and characterization of a conditional mitochondrial complex I assembly system. *J. Biol. Chem.* **279,** 12406–12413
86. Yadava, N., Potluri, P., and Scheffler, I. E. (2008) Investigations of the potential effects of phosphorylation of the MWFE and ESSS subunits on complex I activity and assembly. *Int. J. Biochem. Cell Biol.* **40,** 447–460
87. Chinta, S. J., Rane, A., Yadava, N., Andersen, J. K., Nicholls, D. G., and Polster, B. M. (2009) Reactive oxygen species regulation by AIF- and complex I-depleted brain mitochondria. *Free Radic. Biol. Med.* **46,** 939–947